

Comparison of the wind nowcasting generated by the WRF model and an two LSTM models



Comparación del pronóstico de viento generado por el modelo WRF y dos modelos LSTM

<https://cu-id.com/2377/v29n3e04>

 Maibys Sierra Lorenzo*,  Adrián Fuentes Barrios,  Alfredo E. Roque Rodríguez**,
 Aleida Rosquete Estevez,  Dayanis M. Patiño Avila***

¹ Instituto de Meteorología, La Habana, Cuba

ABSTRACT: Cuba is immersed in the use of wind energy. However, for its development it has required various efforts in different fields, including the improvement of tools that make the wind predictable and, in turn, wind generation, such is the case of very short-term forecasts. For this reason, this paper compares the wind forecast of the Weather Research and Forecasting model (WRF) at 3 km spatial resolution a Long Short-Term Memory (LSTM) model type. The comparison and evaluation of the forecasts of the models is carried out with data from the Gibara I and II wind farms and the Los Cocos wind survey mast, located in Holguín, Cuba, with wind speed measurements every 10 minutes at a height of 50 m. The LSTM were built by first training the observations and then combining the observations with the WRF model forecast. The results of the comparison were carried out for three study cases and indicate that both LSTM models present better results than the WRF model, although the differences do not exceed 1 m/s. However, for the case studies, the WRF model behaves well reproducing the daytime cycle, but with a MAE greater than 4 m/s.

Key Words: wind nowcasting, renewable energy sources, LSTM models, WRF model.

RESUMEN: Cuba se encuentra inmersa en el empleo de la energía eólica. Sin embargo, para su desarrollo ha requerido diversos esfuerzos en diferentes campos, incluyendo el perfeccionamiento de herramientas que hagan predecible el viento y a su vez la generación eólica, tal es el caso de los pronósticos a muy corto plazo. Por tal motivo, en el presente trabajo se compara el pronóstico del viento producido por Weather Research and Forecasting Model (WRF) a 3 km de resolución espacial y un modelo de inteligencia artificial del tipo Long Short Term Memory (LSTM). La comparación y evaluación de los pronósticos de los modelos se realiza con datos de los parques eólicos Gibara I y II y la torre de prospección eólica Los Cocos, ubicadas en la provincia de Holguín, Cuba. Allí se realizan mediciones de la velocidad del viento cada 10 minutos a una altura de 50 m. El LSTM se construyó entrenando primero las observaciones y luego combinándolas con el pronóstico del modelo WRF. Los resultados de la comparación se realizaron para tres casos de estudio e indican que ambos modelos LSTM presentan mejores resultados que el modelo WRF, aunque las diferencias no superan 1 m/s. Sin embargo, para los casos de estudio, el modelo WRF se comporta bien reproduciendo el ciclo diurno, pero con un MAE superior a 4 m/s.

Palabras clave: predicción inmediata del viento, fuentes de energía renovable, modelos LSTM, modelo WRF.

INTRODUCTION

The demand for electricity has increased remarkably worldwide with rapid economic, social and industrial development. The need to mitigate the

impacts of climate change, the serious threat posed by the depletion of non-renewable energy resources, and rising fuel prices have driven growth in the use of renewable energy sources.

*Autor para correspondencia: Maibys Sierra Lorenzo. E-mail: maibysl@gmail.com

**E-mail: alfroquerodriguez@gmail.com

***E-mail: dayanmario212@gmail.com

Received: 13/05/2023

Accepted: 26/06/2023

Conflict of Interest: The authors declare there is no conflict of interest.

Contribution Declaration: Maibys Sierra Lorenz: **Conceptualización, Análisis formal, Investigación, Metodología, Redacción, Redacción - revisión y edición, Validación, Supervisión.** Adrián Fuentes Barrios: **Análisis formal, Metodología, Software, Validación, Visualización.** Alfredo E. Roque Rodríguez: **Adquisición de financiación, Administración de proyecto, Recursos, Redacción - revisión y edición.** Aleida Rosquete Estevez: **Análisis formal, Validación, Redacción - revisión y edición.** Dayanis M. Patiño Avila: **Análisis formal, Validación, Redacción - revisión y edición.**

This article is under license [Creative Commons Attribution-NonCommercial 4.0 International \(CC BY-NC 4.0\)](https://creativecommons.org/licenses/by-nc/4.0/)

Over the past decade, wind power has been one of the fastest growing energy sources in the world. According to the Global Wind Energy Council (GWEC) in April 2022, the wind industry enjoyed its second-best year, with an increase of 93.6 GW of capacity (72.5 GW on land (onshore) and 21.1 GW over the sea (offshore), being, therefore, the total accumulated capacity of 837 GW (GWEC, 2022). All this was possible, even due to the complications caused by Covid 19.

Cuba, on the other hand, as part of the modification of its electricity generation matrix, has not been left behind in the use of this source. By 2030, it is intended to install more than 300 MW (Roque y Yu, 2014), with a coverage of 13 wind farms to deliver this energy production, according to (Rosell, 2015), (Pedraza, 2018). In fact, the generation of electricity from wind energy represented 6% of the country's total electricity in 2020. The total generation of the Gibara I and II wind farms in 2022 was 215 GW/h (Veloz, 2022), which is equivalent to 53,300 tons of unconsumed fuel, so 161,081 tons of carbon dioxide and other polluting gases were stopped from being emitted.

Due to the intermittent nature of wind power, accurate wind speed forecasting becomes essential. The use of prediction tools allows estimating the generation of energy that will be injected into the network, for planning and balancing in real time of the electrical system.

The national electrical energy system must be ready to take over the generation of electrical energy from conventional sources at times when it cannot be produced from wind in order to make adequate and effective use of the wind resource. Wind forecasts are necessary for this in the locations where the wind farms will be installed. The length of these forecasts varies from a few minutes to two hours, which in the literature is known as very short-term forecasts.

In the international sphere, among the methods most used to make these forecasts are statistical methods ranging from classical variants to more advanced variants based on artificial intelligence as exposed by the works of (Carpinone *et al.*, 2015), (Sapronova *et al.*, 2016). Some results have also been reported using Numerical Weather Prediction (NWP) models, persistence method, nearest neighbor method as in the case of (Appice *et al.*, 2015), wavelet basis representation and neural networks according to (Senkal y Ozgonenel, 2013).

There have been many artificial intelligence methods used for wind forecasting in this type of applications as exposed in the works (Senkal y Ozgonenel, 2013), (Schicker *et al.*, 2017), (Mora *et al.*, 2021), (Bouche *et al.*, 2022), (Li *et al.*, 2022), highlighting the Multilayer Perceptron and LSTM types. The success of the forecast methods mentioned, except for the

NWP, depends on the availability of stable and quality observations.

It should also be noted that the ANEMOS project (Giebel *et al.*, 2011), has been one of the investigations that has had great relevance, whose objective was the development of advanced prediction models that substantially improved the tools available to date.

Regarding the national scope, there are some studies where the Weather Research and Forecast (WRF) numerical model, statistical models, and neural networks have also been used to produce short-term wind speed forecasts, such is the case of the works by (Hinojosa, 2015), (Roque *et al.*, 2015a), (Roque *et al.*, 2015b), (Martínez y Roque, 2019). Only (Martínez y Roque, 2019) handled very short-term forecasting and produced the projections using actual data. Particularly in Cuba, a variety of circumstances, including power outages, communication issues, storage issues, and more, pose a threat to getting observations in real time. A forecast system based only on these measurements would be equally unstable in light of their inherent instability. The above issues motivated us to launch this inquiry, which uses real data as well as the WRF model's projection so that it can be used as an alternative in the event of a measurement failure. In a first approximation, the available the WRF model outputs whose temporary frequency is every 1 hour were used, so the data every 10 min were obtained by interpolating, as in (Fuentes *et al.*, 2022). Despite this limitation, the results were encouraging, so in this update, the experiments with the WRF model were repeated, generating the outputs every 10 minutes for the period February 1, 2019 to January 31, 2020, coinciding with the available observations. The previously obtained LSTM models were recalibrated with the new data and the comparison was made. As a result, a better ability of the LSTM models is reaffirmed, however the forecasts with the WRF model did not have errors greater than 1 m/s and the diurnal cycle was adequately represented. The document is organized as follows, after the introduction the materials and methods used are described, a description of the area and the case studies, as well as the method of extrapolation of the wind speed at height are presented. Next, the analysis of the results is presented, then the conclusions, and the literature consulted.

MATERIALS AND METHODS

Study region

The study area is located in the Gibara municipality (Figure 1), in the province of Holguín, where this wind resource has been tested for its exploitation in large scale electricity production. Said area was selected as part of the national project: Improvement of the Energy Forecast System for Wind and Photovoltaic farms.

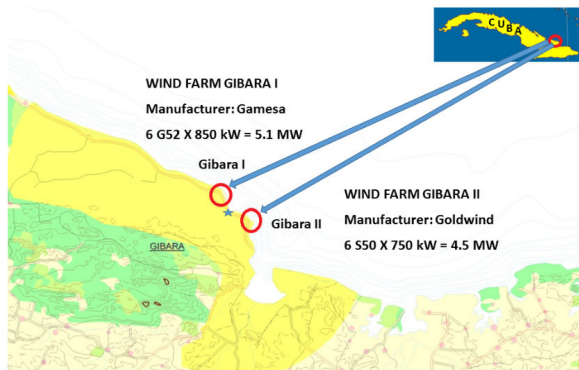


Figure 1. Location of the Gibara I and II wind farms in the province of Holguín and the Los Cocos wind survey mast. *Note:* Taken from (Roque *et al.*, 2022).

Two wind farms are located in this territory, Gibara I from the manufacturer GAMESA (now GAMESA-Siemens), has a power of 5.1 MW and Gibara II from the manufacturer GOLDWIND, with a power of 4.5 MW; each of these has six wind turbines.

Close to the parks, the Los Cocos wind survey mast is located 300 meters from the coastline and has a height above sea level of 3 meters (Roque, 2015).

Data Used

One-year wind speed observations were gathered from Los Cocos wind survey mast, for the creation of very short-term wind forecasts. The duration was from February 1 through January 31 of 2020. At this tower, wind measurements were taken every 10 minutes at heights of 10, 30, 50, and 100 m, these measurements represent the mean value of the wind. Just the findings from the measurements taken at a 50 m height are displayed in this paper.

Sistema de Pronóstico Inmediato (SisPI)

The SisPI is a system that predicts the different meteorological events in the short term, with a range of 24 hours. It is initialized with data from the Global Forecast System (GFS), and configured with the Weather Research and Forecasting (WRF) atmospheric model. It also has four daily updates every six hours (0000, 0600, 1200 and 1800 UTC), and three domains with a resolution of 27, 9 and 3 km (Sierra *et al.*, 2015), (Sierra *et al.*, 2017).

Precisely, the numerical forecasts were derived from the Short-Range Prediction System (SisPI)'s 3km resolution simulation domain (see Figure 2).

Unlike the previous work (Fuentes *et al.*, 2022), the SisPI outputs were taken every 10 minutes at a

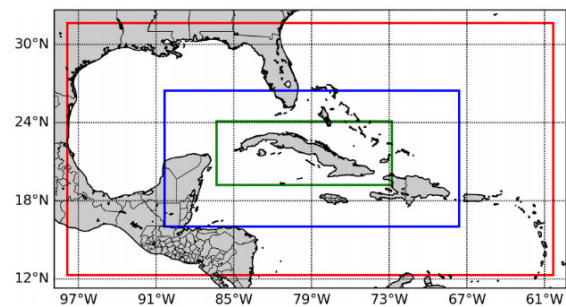


Figure 2. SisPI simulation domains. The study's 3km resolution zone is represented by the green square. *Note:* (Source: self-made)

height of 10 m to then extrapolate the wind at a height of 50 m. The extrapolation was based on the results obtained by (Roque *et al.*, 2015a) in previous investigations, where the well-known wind power law equation (Emeis, 2013), expressed as follows in (1) was used,

$$u(z) = u_r \left(\frac{z}{z_r} \right)^\alpha \quad (1)$$

where α is the coefficient of vertical variation of the wind or Hellmann's exponent, u_r is the reference wind speed at height z_r , usually 10 m. The values of α found by (Roque *et al.*, 2015a), for the location of the Los Cocos survey mast are shown in Table 1.

For both data sources, sets of 12 inputs every 10 min were generated to forecast 12 outputs also every 10 min with a 2-h forecast horizon. With this set of data, we proceeded to train the LSTM-type neural network models.

Long Short-Term Memory (LSTM)

The basic configuration of the LSTM models is shown in Figure 3. As input data for the training, only the tower data were taken for the LSTM-1 model, and for the LSTM-2 model, also was used the forecasts of the WRF model as core of SisPI.

The prediction is obtained by supplying the input data to a deep neural network. This network consists of a first LSTM layer with 64 units, followed by another with 32 units. The dropout technique is also applied after each LSTM layer to control overfitting. Finally, a final dense layer with simple unit and linear activation provides a final probability.

To get a proper prediction, this network must be trained. Training is an iterative learning process in which data instances (a segment of inputs) for which the correct output are known (whether or not there will be a sharp increase in wind speed in the near future). These are presented to the network one at a time, each

Table 1. Values of the wind power law exponent for each type of stability in the location of the Los Cocos survey mast. *Note:* Taken from (Roque *et al.*, 2015a).

	Unstable	Neutral	Stable
α	0.09	0.10	0.16

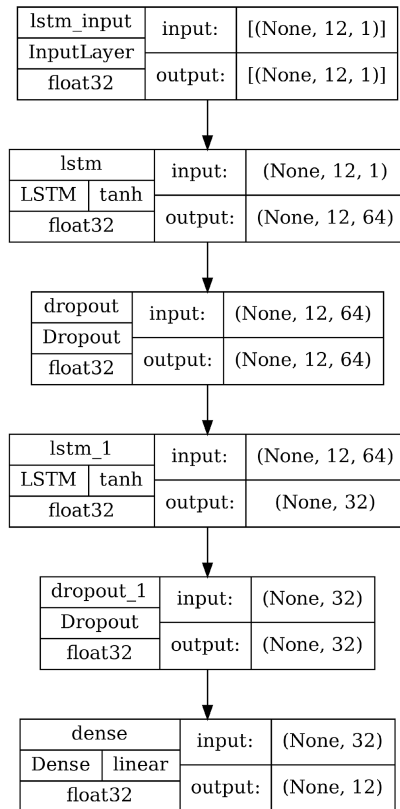


Figure 3. Basic LSTM configuration. Note: (Source: self-made)

time adjusting the weights associated with the input values in each layer. The process is repeated multiple times with different batches of input data until the weights fit well enough to predict the correct label (or probability) for any given input sample. To create the training data instances, a time series is recorded for each wind turbine over a long period of time. From this data set segments of the appropriate size are extracted. These segments can be tagged, as subsequent entries can be checked for an increase. This set is used to train the weights in the deep network. The set will consist of positive (cases in which the prediction must be positive, that is, there will be a high increase) and negative (no increase should be predicted) instances.

In addition to the validation set, three case studies (28 May 2019, 2 August 2019, and 18 November 2019) representing various wind regimes were left out of the training for the evaluation. These case

studies correspond to different months of the year. These days were chosen regardless of the types of synoptic situation prevailing during the study period, rather they were selected in terms of the mean value of the wind, that is, a day with a favorable wind speed, and others where the speed is not very eminent. The first two cases correspond to the rainy season of the year (Table 2), the synoptic situation that prevailed in those days responds to the influence of the subtropical anticyclone of the Atlantic, and it is precisely during the rainy season where it reaches its highest frequency. The last case belongs to the dry season, this day a quasi-stationary front was found prevailing, this system responds to the type of synoptic situation of Frontal Systems (Soler et al., 2020), which usually have their highest frequency precisely during the dry season of the year.

Table 2, shows the selected days with a brief description of the synoptic characteristics and Figure 4 presents the synoptic map for each case.

Metrics Uses

To carry out the analysis, several statisticians were calculated, such as:

The mean absolute error (MAE), as shown in (2), is defined as the absolute difference between the predicted and observed values, with a range of values between zero and infinity, with the optimal forecast being when it reaches zero.

The root means square error (RMSE), as shown in (3), is a measure of error that is defined as the root mean square error (MSE).

The Pearson correlation coefficient (r), as shown in (4), describes the linear strength of the relationship between predicted and observed values. The value of the coefficient r is between: $-1 \leq r \leq 1$. A value of $r = 0$ means that there is no linear correlation between the variables studied.

$$MAE = \frac{\sum_{i=1}^n (O_i - F_i)^2}{n} \quad (2)$$

$$RMSE = \sqrt{\frac{1}{n} \sum_{i=1}^n (O_i - F_i)^2} \quad (3)$$

$$r = \frac{\sum_{i=1}^n (O_i - \bar{O})(F_i - \bar{F})}{\sqrt{\sum_{i=1}^n (O_i - \bar{O})^2 \sum_{i=1}^n (F_i - \bar{F})^2}} \quad (4)$$

Table 2. Study cases and synoptic description. Note: (Source: self-made)

Day	May 28, 2019	August 2, 2019	November 18, 2019
Synoptic description	It was characterized by the influence of a "disturbed" extended oceanic anticyclonic flow (Figure 3a). The wind speed values in the Los Cocos survey mast were 4.5 m/s on average at a level of 50 m above the surface with a maximum of 5.8 m/s and an average minimum of 3.1 m/s. This average behavior did not ensure a good performance of the wind farms.	It was characterized by the influence of an "undisturbed" extended oceanic anticyclonic flow in the eastern half (Figure 3b). Another day with wind energy conditions similar to the previous one, but with another synoptic situation. The wind speed values in the Los Cocos survey mast were 3.6 m/s on average at a level of 50 m above the surface, with a maximum of 4.8 m/s and an average minimum of 2.4 m/s.	It was characterized by the influence of a quasi-stationary front over Cuba (Figure 3c). Day characterized by the lowest mean values of wind speed of those selected (3.6 m/s) whose maximum values averaged 4.8 m/s and the minimum 2.4 m/s.

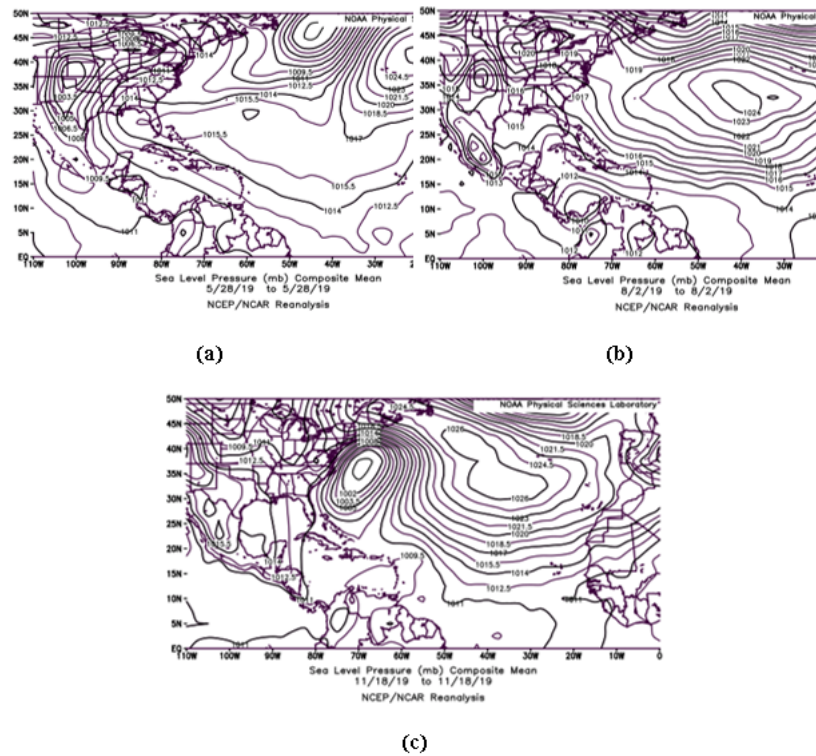


Figure 4. Configuration of the surface pressure field for: (a) May 28, 2019, (b) August 2, 2019 and (c) November 18, 2019. *Note:* Taken from the web site: www.esrl.noaa.gov/psd/.

Where O_i is the observed value and F_i is the forecast value at time i of the different models used.

RESULTS

Figure 5 exhibits, as a result of the behavior of the mean absolute error that was acquired when forecasting 12 periods separated every 10 minutes using the data subset used for LSTM-1 and LSTM-2 model training validation. The red line represents the result with the data from Los Cocos survey mast (LSTM-1) the blue line corresponds to the results of training the LSTM with the SisPI forecast and the observation tower (LSTM-2), the black line represents the forecast produced by the WRF model.

As can be seen in said figure the MAE increased for all three models as the prediction went away from the initial terms, the LSTM-1 model has an oscillation around 0.3 m/s and 0.7m/s, the LSTM-2 model, comprises values close to 0.4 m/s and 0.5 m/s, quite good, while the WRF model reaches higher values, between 0.9 m/s and 1 m/s approximately.

It can be seen that, on average, the errors of the three models do not exceed 1 m/s, which is very favorable. Note that the LSTM-type models had lower errors in relation to the SisPI, which indicates good performance on their part.

Another aspect that stands out, is how remarkable is the ability of the LSTM-2 model to correct the WRF forecast model. The combination of both data sources results in a forecast very similar to that obtained with

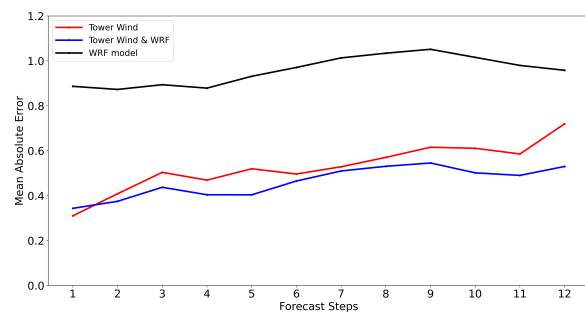


Figure 5. Behavior of the MAE for the 12 forecast terms of the validation set. The blue line refers to the results of training the LSTM with the SisPI forecast and the tower observations (LSTM-2), the black line represents the forecast produced by the WRF model, and the red line shows the results acquired using data from the Torre Los Cocos (LSTM-1). *Note:* (Source: self-made)

the LSTM-1 model. In fact, the LSTM-2 model even reaches lower MAE values than the LSTM-1 model.

As a form of verification, let's see the results obtained for the selected case studies.

Verification of the Study Cases

The results obtained for the selected study cases are summarized in Table 3 where the values of the evaluation metrics used are observed. Note that in the case of LSTM-type models, there is consistency with the results achieved with the validation set. Both neural network models presented a MAE below 0.5 m/s for all cases, the RMSE was close to zero with values

Table 3. Evaluation of the forecasts of the LSTM and WRF models in the case studies. (Source: self-made)

Metrics	28 May 2019			2 August 2019			18 November 2019		
Model	LSTM-1	LSTM-2	WRF	LSTM-1	LSTM-2	WRF	LSTM-1	LSTM-2	WRF
MAE	0.49	0.45	2.43	0.25	0.36	1.6	0.15	0.28	0.94
Pearson correlation	0.99	0.99	-0.57	0.99	0.99	0.27	0.99	0.98	-0.01
RMSE	0.35	0.28	9.55	0.18	0.27	4.22	0.04	0.12	1.34

not greater than 0.4 m/s, while the Pearson correlation coefficient was 0.9 in the three days. These metric values correspond to what is observed in Figure 5, where the similarity between the LSTM-type forecasts and the measurements in the tower is observed.

On the other hand, the results with the WRF model indicate a deficiency of the model, since the lowest MAE was 0.94 m/s for November 18, reaching its highest value of 2.43 m/s for May 28, 2019. The highest RMSE was also obtained for the same day with 9.55 m/s, which indicates that in particular for the prevailing synoptic situation, the model fails to adequately represent the behavior of the wind.

As a preliminary conclusion, this first analysis suggests that in the absence of actual data, the WRF model forecast can be used as an alternative.

Figure 6 shows the behavior of the diurnal wind cycle, using the LSTM models and the WRF model for the three cases analyzed. The red line indicates the behavior of the observed wind. The black line represents the WRF model, where it can be seen that there is no correspondence, especially in the afternoon hours. On the other hand, the blue line represents the behavior of the LSTM-1 model trained only with the observations; the green line to the LSTM-2 model, which uses as input the observations and the forecast

given by the SisPI; As can be seen, both models have a behavior very similar to that of the observations.

It should be noted that in the case of the WRF model, the initial growth of the curves in the first forecast hour is due to the well-known "spin up" of the model, which indicates the heating phase of the model, that is, it is the time simulation required for the model to achieve physical equilibrium and, regardless of the initial conditions imposed on it, produce its own internal variability.

DISCUSSION

As seen in figure 5, despite the fact that the LSTM-1 model has a fairly good MAE, which does not exceed 0.8 m/s; the LSTM-2 model is the one that showed the best results, with a MAE of just under 0.6 m/s, which suggests that the WRF model forecasts provide some dynamic and physical consistency that complements the observations. Therefore, a variant could be to use the information from the measurements to apply a bias correction to the numerical forecasts.

Regarding the verification of the cases studied for the WRF model, it was possible to observe, as shown in Table 2, that for November 18, the values of the

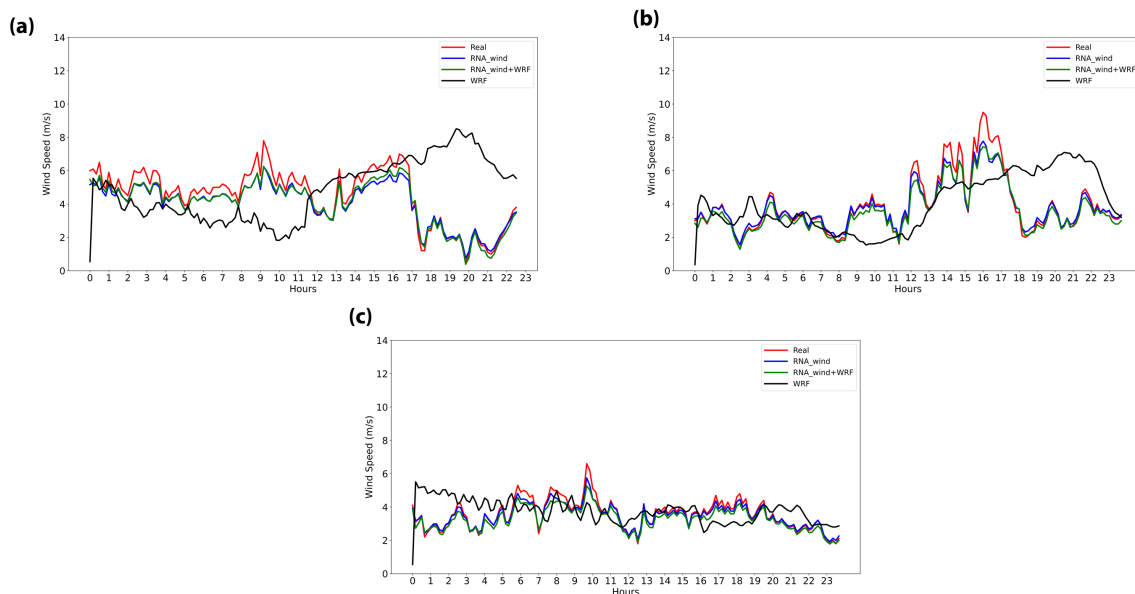


Figure 6. Forecast wind values for each of the case studies: 28 May 2019 (a), 2 August 2019 (b) and 18 November 2019 (c); using the LSTM-1 (RNA wind, yellow line), the LSTM-2 model (RNA_wind+WRF), green line) and, the WRF forecast model (WRF, black line). The red line represents the observed wind behavior. *Note:* (Source: self-made)

metrics were relatively better compared to the rest of the cases. During this day, the prevailing synoptic situation was a quasi-stationary front, however, the influence of this situation itself has low frequency for our country.

Regarding August 22, the values of the statistics did not turn out to be so favorable. That day, the weather was under the presence of an undisturbed extended oceanic anticyclonic flow, which responds to the influence of the North Atlantic Subtropical Anticyclone.

However, May 28 was the day that produced the highest results, and in turn, the most unfavorable. This day the weather in Cuba was influenced by the presence of an extended and disturbed oceanic anticyclonic flow, a situation that, as on August 22, responds to the presence of the Subtropical North Atlantic Anticyclone, and as is known, this system is predominant during almost the whole year and imposes the trade winds that are preeminent throughout the country. This could be related to the SisPI has deficiencies to represent the correct position of the subtropical dorsal, with a tendency to predict a drier tropospheric column compared to the actual one, according to (Paula *et al.*, 2022), This study evaluated the ability of the SisPI to represent the subtropical anticyclone of the North Atlantic over the external domain during the 2020 rainy season).

Also, in the work of (Paula *et al.*, 2022), it was found that the SisPI shows tendencies to locate the high geopotential zones further south of their actual position, which produces changes in the forecast synoptic flow. And that the errors of this present a maximum in the month of May.

This may be the cause of the limitations of the WRF model with the SisPI configuration to adequately forecast the wind.

As could be seen in figure 6, the LSTM models represent the daytime cycle quite well, however the WRF model does not correspond to it, where the measurements indicate a decrease in speed and the WRF model predicts an increase in values. of the variable. Hence, no correlation is found between what is predicted and what is observed. Despite the limitations of the WRF model, if an LSTM model is used to correct the errors, a very good forecast is achieved, so it is recommended to use the combination of both data to make the forecast.

CONCLUSIONS

From the results presented, we can arrive at the following conclusions:

The LSTM models demonstrate a very strong ability to anticipate wind force using both the data from Los Cocos survey mast and the combination of the same data with the SisPI forecasts.

Although the MAE and RMSE of the forecasts utilizing the SisPI data are slightly greater, they can be corrected using an LSTM-type model.

Despite the appointed difficulties of SisPI configuration, in the absence of observations, it is possible to use the SisPI data with bias correction as an alternative for very short-term wind forecasting.

REFERENCES

- Appice, A., Prasilovic, S., Lanza, A., y Malerba, D. (2015). Very short-term wind speed forecasting using spatio-temporal lazy learning. In *Discovery Science: 18th International Conference, DS 2015, Banff, AB, Canada, October 4-6, 2015. Proceedings 18*, 9-16. Springer International Publishing. DOI https://doi.org/10.1007/978-3-319-24282-8_2.
- Bouche, D., Flamary, R., d'Alché-Buc, F., Plougonven, R., Clausel, M., Badosa, J., y Drobinski, P. (2022). Wind power predictions from nowcasts to 4-hour forecasts: a learning approach with variable selection. DOI <https://doi.org/10.1016/j.renene.2023.05.005>.
- Carpinone, A., Giorgio, M., Langella, R., y Testa, A. (2015). Markov chain modeling for very-short-term wind power forecasting. *Electric power systems research*, 122, 152-158. ISSN 0378-7796. DOI <https://doi.org/10.1016/j.epsr.2014.12.025>.
- Council, G. W. E. (2022). Global wind report 2021. *Global Wind Energy Council*.
- Emeis, S. (2013). Atmospheric Physics for Wind Power Generation. ISBN 978-3-319-72859-9. DOI <https://doi.org/10.1007/978-3-319-72859-9>.
- Fuentes, A., Sierra, M., y Roque, A. (2022). LSTM Model for Wind Speed and Power Generation Nowcasting. *Environmental Sciences Proceedings*, 13(1), 30. ISSN: 2664-0880.
- Giebel, G., Draxl, C., Brownsword, R., Kariniotakis, G., y Denhard, M. (2011). The state-of-the-art in short-term prediction of wind power. A literature overview, 2nd Edition G. Advanced Tools for the Management of Electricity Grids with Large-Scale Wind Generation. ANEMOS Project, Specific Targeted Research Project Contract N°: 038692. 2011.
- GWEC: Global Wind Energy Council. 2021. Global Wind Report. [Cited: 18, may, 2023]. Available in: <https://gwec.net/greenrecovery/>.
- Hinojosa, M. (2015). *Pronóstico de Viento a Muy Corto Plazo Para Parques Eólicos*. Bachelor's Thesis, University of Havana, Habana, Cuba.
- Li, Z., Luo, X., Liu, M., Cao, X., Du, S., y Sun, H. (2022). Short-term prediction of the power of a new wind turbine based on IAO-LSTM. *Energy Reports*, 8, 9025-9037. DOI <https://doi.org/10.1016/j.egy.2022.07.030>.

- Martínez, B., y Roque, A. (2019). Pronóstico energético a muy corto plazo para el Parque Eólico Gibara I utilizando un modelo autorregresivo. *Revista Cubana de Meteorología*, 25(2). ISSN: 0864-151X.
- Mora, E., Cifuentes, J., y Marulanda, G. (2021). Short-term forecasting of wind energy: A comparison of deep learning frameworks. *Energies*, 14(23), 7943. DOI <https://doi.org/10.3390/en14237943>.
- Paula, J., Sierra, M., y González, P. (2022). Analysis of SisPI Performance to Represent the North Atlantic Subtropical Anticyclone. *Environmental Sciences Proceedings*, 19(1), 40. DOI <https://doi.org/10.3390/ecas2022-12804>.
- Pedraza, J. (2018). Renewable energy sources in Cuba: Current situation and development prospects. *Focus on Renewable Energy Sources*, (August), 49-104. [Cited: 18, may, 2023]. Available in: <https://www.researchgate.net/publication/326698092>.
- Roque, A. 2015. Estudio comparativo de estaciones de prospección eólica, con respecto a la torre de referencia meteorológica de El Ramón, en Holguín. *Revista Ecosolar*, ISSN: 1028 - 6004, La Habana, Cuba.
- Roque, A., Borrajero, I., Hernández, A., y Sierra, M.(2015a). *Short-term energy forecast for the Gibara I and Los Canarreos wind farms*. Instituto de Meteorología de Cuba, Havana, Cuba. Technical Report. P211LH003 - 004.
- Rodríguez, A., Hernández, A., Lorenzo, M., y Montejo, I. (2022). Pronóstico numérico a corto plazo de la rapidez del viento para los parques eólicos de Gibara I y II. *Revista Cubana de Meteorología*, 28(2). ISSN: 2664-0880.
- Roque, A., Sierra, M., Borrajero, I., y Ferrer, A. (2015b). *Short-term wind forecast in meteorological reference towers for the Cuban wind program*. Instituto de Meteorología de Cuba, Havana, Cuba. Technical Report
- Roque, A. y Yu, W. (2014). *Informe Científico Técnico del Proyecto Atlas Eólico de Cuba*. Instituto de Meteorología de Cuba, Havana, Cuba. Technical Report.
- Rosell, D. (2015, 25-28 May). “Desarrollo de las Fuentes Renovables de Energía” [Conferencia Magistral]. In Proceedings of the Congreso Internacional de Energía Renovable, Ahorro y Educación Energética. Palacio de Las Convenciones, La Habana, Cuba.
- Sapronova, A., Meissner, C., y Mana, M. (2016, September). “Short time ahead wind power production forecast. In *Journal of Physics: Conference Series*”. 749, (1), 012006. IOP Publishing. DOI [10.1088/1742-6596/749/1/012006](https://doi.org/10.1088/1742-6596/749/1/012006).
- Schicker, I., Papazek, P., Kann, A., y Wang, Y. (2017, April). “Wind speed and wind power short and medium range predictions for complex terrain using artificial neural networks and ensemble calibration”. In *EGU General Assembly Conference Abstracts*, 11846.
- Senkal, S., y Ozgonenel, O. (2013, November). “Performance analysis of artificial and wavelet neural networks for short term wind speed prediction”. In *2013 8th International Conference on Electrical and Electronics Engineering (ELECO)*, 196-198. IEEE. DOI: [10.1109/ELECO.2013.6713830](https://doi.org/10.1109/ELECO.2013.6713830).
- Sierra, M., Borrajero, I., Ferrer, A., Morfá, Y., Morejón, Y., y Hinojosa, M. (2017). *Estudios de sensibilidad del SisPI a cambios de la PBL, la cantidad de niveles verticales y, las parametrizaciones de microfísica y cúmulos, a muy alta resolución. Informe de resultado Instituto de Meteorología, La Habana, Cuba*. DOI:[10.13140/RG.2.2.29136.00005](https://doi.org/10.13140/RG.2.2.29136.00005). [Cited: 18, may, 2023]. Available in: <https://www.researchgate.net/publication/325050959>.
- Sierra, M., Ferrer, A., Hernández, R., González, G., Cruz, R., Borrajero, I., Rodríguez, C.; Rodríguez, N., y Roque, A. (2015). *Sistema Automático de Predicción a Mesoescala de Cuatro Ciclos Diarios. Informe de resultado Instituto de Meteorología, La Habana, Cuba*. DOI: [10.13140/RG.2.1.2888.1127](https://doi.org/10.13140/RG.2.1.2888.1127). [Cited: 18, may, 2023]. Available in: <https://www.Researchgate.net/publication/281555728>.
- Soler, E., Lecha, L., Sánchez, L., y Naranjo, Y. (2020). *Catálogo de los tipos de situaciones sinópticas que influyen sobre Cuba*. Nueva Gerona, Isla de la Juventud: Centro Meteorológico de la Isla de la Juventud, INSMET. DOI:[10.13140/RG.2.2.12542.20802](https://doi.org/10.13140/RG.2.2.12542.20802).
- Veloz, G. (2022, 26 agosto). Propósito claro: generar electricidad porque el país lo necesita. *Revista Granma*. [Cited: 18, may, 2023]. Available in: <https://www.granma.cu/cuba/2022-08-26/proposito-claro-generar-electricidad-porque-el-pais-lo-necesita-26-08-2022-23-08-30>.